Frequency Domain Image Restoration:

Parameter K (NSR) and Gain of Wiener Filter vis-à-vis Length and Direction of Motion Blur

Abdul Rasak Zubair

Electrical/Electronic Engineering Department
University of Ibadan
Ibadan, Nigeria
Email: ar.zubair [AT] ui.edu.ng

Abstract—**Imperfection of Imaging systems and environmental effects cause images to be degraded by blurring and noise. Blurring due to relative motion between imaging system and object is simulated. Image restoration in the frequency domain by Wiener filter is implemented. The parameters of motion blur, length and direction, are varied. The parameter K (NSR-Noise to Signal Ratio) and Gain of Wiener filter are evaluated. The quality of restored images is also observed and recorded. The study is carried out with six test images. With parameter K set to zero, the Wiener filter is put into inverse filter mode; Gain is negative in all cases and quality and appearance of restored images are very poor. Clear images are obtained with K > 0. Wiener filter's Gain increases as K increases from 0 to a value termed 'Optimum K' when the Gain is maximum; the Gain reduces with further increase in K. Motion blur functions of the same length but opposite directions are equivalent as they have same values of Optimum K and Gain at Optimum K. With constant motion blur length, Wiener filter's Optimum K and Gain at Optimum K rise and fall rhythmically as motion blur direction varies from 0° to 180°. With constant motion blur direction, Wiener filter's Optimum K and Gain at Optimum K decrease as motion blur length increases from 2 pixels to 15 pixels.**

Keywords-degradation; Wiener filter restoration; motion blur parameters; noise to signal ratio; Gain;

I. INTRODUCTION

Environmental effects and imperfections in the imaging system can cause the recorded images to be degraded by blurring and noise [1,2,3,4,5,6]. Blurring is present in any imaging system which uses electromagnetic radiation; for example, visible light and x-rays. Diffraction limits the resolution of an imaging device to features on the order of the illuminating wavelength.

Scattering of light between the target object and imaging system by the atmosphere introduces additional blurring. Lenses and mirrors cause blurring because they have limited spatial extent and optical imperfections. Discretization results in yet more blurring because devices such as CCDs average illumination over regions rather than sampling it at discrete points. Relative motion between the camera and object is also another cause of image blurring.

Noise is similarly omnipresent: any imaging device must use a finite exposure time, which introduces stochastic noise from the random arrival of photons. Optical imperfections and instrumentation noise such as thermal noise in CCD devices result in more noise. Sampling causes noise due to aliasing of high-frequency signal components and digitization produces quantization errors. Further noise can be introduced by communication errors and compression.

Image restoration (sometimes known as deblurring or deconvolution) is the process of reconstructing or estimating the true image from the degraded one [8,9,10,11,12,13,14,15]. A criterion of goodness that will yield some optimal estimate of the true image is formulated for the restoration process [16,17,18].

Restoration is an inverse problem [17]. Whereas the forward problem has a unique solution, because of the causality principle, the inverse problem may have many solutions - when different models of the system predict similar observations, or no solution at all (inconsistent data). This is why a special mathematical theory exists that formalizes inverse problems [17,19,20,21].

Image restoration is an area that also deals with improving the appearance of an image. It can be seen as a special kind of image enhancement [22]. However, unlike enhancement, which is subjective, image restoration is objective, in the sense that restoration techniques tend to be based on mathematical or probabilistic models of image degradation. Enhancement, on the other hand, is based on human subjective preferences regarding what constitutes a "good" enhancement result. The goal of enhancement is to produce the most visually pleasing image starting from a recorded image. The goal of restoration is to produce the best possible estimate of the original image starting from a recorded image. The goal of enhancement is beauty; the goal of restoration is truth.

Wiener filter is the Mean Square Error (MSE) optimal frequency domain restoration filter for images degraded by additive noise and blurring. Wiener filter has an important parameter K which represents Noise to Signal Ratio (NSR) and Gain. Gain is measured in dB. Image restoration in general and Wiener filtering in particular are active areas of research in satellite remote sensing, medical and scientific imaging [23,24,25,26,27,28,29,30,31,32,33,34,35].

The operation of Wiener filter is studied extensively in this work with motion blur and with the aid of six test images. Motion blur has two parameters; length (L pixels) and direction (Angle θ degrees). The dependency of Wiener filter's parameter K (NSR), Gain and restoration quality on motion blur length L and direction θ is investigated.

II. METHOD

A. Image Degradation Model

Fig. 1 shows the degradation model. When an object is being imaged, the acquired (or observed) image, g(m,n) is usually not the same as the true image f(m,n). h(m,n) is the blurring function or Point Spread Function (PSF) of the imaging system. The PSF is the output of the imaging system for an input point source. h(m,n) represents the environmental effects and imaging system imperfections. η(m,n) is an additive noise from the surroundings.
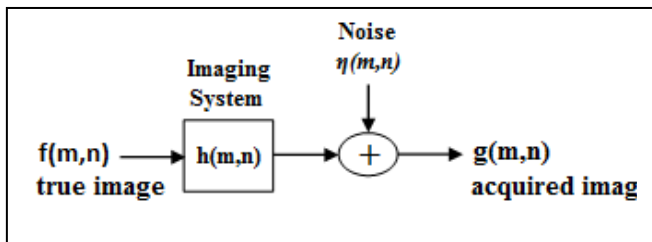

Figure 1. Degradation Model.

In many instances, the acquired (or observed) image g(m,n) can be modelled as two-dimensional convolution of the true image f(m,n) and the point-spread function (also called the blurring function) h(m,n) of a linear shift-invariant system plus some additive noise η(m,n) [1,2,3,11,35] as described by (1) and (2).

$$g(m,n) = h(m,n) \otimes f(m,n) + \eta(m,n) \quad (1)$$

where $\otimes$ is the convolution operator.

$$G(u,v) = H(u,v)F(u,v) + \overline{\eta}(u,v) \quad (2)$$

where H(u,v) is the Optical Transfer Function (OTF) and is the Discrete Fourier Transform of h(m,n), G(u,v) is the Discrete Fourier Transform of the acquired image g(m,n) and $\overline{\eta}(u,v)$ is the Discrete Fourier Transform of the noise η(m,n).

Discrete Fourier Transform pair for a sampled array f(m,n) of dimensions M by N to a frequency array F(u, v) are given by (3) and (4) [1,2,3,5,7].

$$F(u,v) = \frac{1}{MN} \sum_{m=1}^{m=M} \sum_{n=1}^{n=N} f(m,n) e^{-j2\pi\left(\frac{um}{M}+\frac{vn}{N}\right)} \quad (3)$$

$$f(m,n) = \sum_{u=1}^{u=M} \sum_{v=1}^{v=N} F(u,v) e^{j2\pi\left(\frac{um}{M}+\frac{vn}{N}\right)} \quad (4)$$

The task of image restoration is to solve (1) for f(m,n) in the spatial domain or (2) for F(u,v) in the frequency domain. Solution of (2) with the Minimum Mean Square Error criterion leads to (5) [1,4,5,6,7,16,17,18,27,29,33].

$$F_e(u,v) = \frac{H^*(u,v)G(u,v)}{H^*(u,v)H(u,v) + \dfrac{S_{\eta\eta}(u,v)}{S_{ff}(u,v)}} \quad (5)$$

where $S_{\eta\eta}(u,v)$ and $S_{ff}(u,v)$ are the noise and true (ideal) image power spectra respectively.

The estimate of the true image otherwise called restored image $f_e(m,n)$ is the inverse Fourier transform of $F_e(u,v)$. The restoration filter is known as Wiener Filter and is illustrated in Fig. 2. It has the transfer function as in (6). Most often, noise to signal ratio ($S_{\eta\eta}/S_{ff}$) is unknown and is represented by a constant K as in (7). K is referred to as Noise to Signal Ratio (NSR) and is a key parameter of Wiener filter.

$$T_r = \frac{F_e(u,v)}{G(u,v)} = \frac{H^*(u,v)}{H^*(u,v)H(u,v) + \dfrac{S_{\eta\eta}(u,v)}{S_{ff}(u,v)}} \quad (6)$$

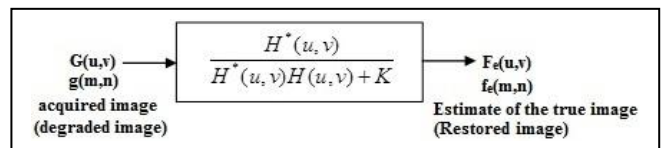$$F_e(u,v) = \frac{H^*(u,v)G(u,v)}{H^*(u,v)H(u,v) + K} \quad (7)$$

Figure 2. Wiener Restoration Filter.

When K=0, the Wiener filter becomes an Inverse Filter as in (8) and (9). The Inverse Filter of a blurred image is a highpass filter. The parameter K of the Wiener filter is related to the low frequency aspect of the Wiener filter. The Wiener filter behaves as a bandpass filter, where the highpass filter aspect is due to the inverse filter and the lowpass filter aspect is due to the parameter K (NSR).

$$F_e(u,v) = \frac{G(u,v)}{H(u,v)} \quad (8)$$

$$T_r = \frac{1}{H(u,v)} \quad (9)$$

B. Motion Blur Model

A physical model is often used to obtain the PSF. Some degradation processes can be easily expressed mathematically (convolution) and also restored simply in images. One of the possible causes of degradation is relative motion between the camera and the object [6,28]. The PSF for a camera with mechanical shutter is given as in (10).

$$h(m,n) = \frac{1}{L} \quad \text{if} \quad \sqrt{m^2 + n^2} \leq \frac{L}{2} \quad \text{and} \quad \frac{m}{n} = -\tan\theta \quad (10)$$
$$0 \quad \text{elsewhere}$$

where $L = v\tau$ is the length of motion during exposure; τ is the period of exposure; v is the relative motion of the scene with respect to the camera along a direction at angle θ with the horizontal axis [6].

Matlab code *fspecial('motion',L,θ)* is used to simulate motion blur with length L and angle θ. The code returns a blurring function h(m,n) to approximate, once convolved with an image, the linear motion of a camera by L pixels, with an angle of θ degrees in a counter-clockwise direction [36,37]. The filter becomes a vector for horizontal and vertical motions. Tables I to IV illustrate some motion blur functions obtained with Matlab code *fspecial('motion',L,θ)*. All elements in a blurring function sum up to 1. The dimensions of the blurring function depend on L and θ.

TABLE I.   MOTION BLUR FUNCTION WITH LENGTH 5 AND ANGLE 30

	Column 1	Column 2	Column 3	Column 4	Column 5
Row 1	0.0000	0.0000	0.0268	0.1268	0.1464
Row 2	0.0000	0.1000	0.2000	0.1000	0.0000
Row 3	0.1464	0.1268	0.0268	0.0000	0.0000

L=5 pixels and angle θ=30° {*h(m,n)=fspecial('motion',5,30)*}; 3 x 5 Matrix.

TABLE II.   MOTION BLUR FUNCTION WITH LENGTH 5 AND ANGLE 0

	Column 1	Column 2	Column 3	Column 4	Column 5
Row 1	0.2	0.2	0.2	0.2	0.2

L=5 pixels and angle θ=0° {*h(m,n)=fspecial('motion',5,0)*}; 1 x 5 Matrix.

TABLE III.   MOTION BLUR FUNCTION WITH LENGTH 4 AND ANGLE 90

	Column 1
Row 1	0.1250
Row 2	0.2500
Row 3	0.2500
Row 4	0.2500
Row 5	0.1250

L=4 pixels and angle θ=90° {*h(m,n)=fspecial('motion',4,90)*}; 5 x 1 Matrix.

C. Motion Blur Simulation

A blurring function h(m,n) with length L and angle θ is simulated. h is a MH x NH matrix. If f is an rgb colour image, f is a MF x NF x 3 matrix. The acquired image g is a MG x NG x 3. The dimensions are related as in (11) and (12).

TABLE IV.   MOTION BLUR FUNCTION WITH LENGTH 10 AND ANGLE 60

	Column 1	Column 2	Column 3	Column 4	Column 5	Column 6	Column 7
Row 1	0.0000	0.0000	0.0000	0.0000	0.0000	0.0730	0.0242
Row 2	0.0000	0.0000	0.0000	0.0000	0.0365	0.0766	0.0000
Row 3	0.0000	0.0000	0.0000	0.0000	0.0864	0.0267	0.0000
Row 4	0.0000	0.0000	0.0000	0.0499	0.0633	0.0000	0.0000
Row 5	0.0000	0.0000	0.0134	0.0998	0.0134	0.0000	0.0000
Row 6	0.0000	0.0000	0.0633	0.0499	0.0000	0.0000	0.0000
Row 7	0.0000	0.0267	0.0864	0.0000	0.0000	0.0000	0.0000
Row 8	0.0000	0.0766	0.0365	0.0000	0.0000	0.0000	0.0000
Row 9	0.0242	0.0730	0.0000	0.0000	0.0000	0.0000	0.0000

L=10 pixels and angle θ=60° {*h(m,n)=fspecial('motion',10,60)*}; 9 x 7 Matrix.

$$MG = MF + MH - 1 \quad (11)$$

$$NG = NF + NH - 1 \quad (12)$$

h(m,n) of dimension MH x NH is transformed to frequency domain as H(u,v) of dimension MG x NG using the Matlab code *fft2* (Two-dimensional discrete Fourier Transform) as in (13). Each of the three colour components of f (MF x NF x 3) is transformed to frequency domain as F(u,v) of dimension MG x NG using Matlab code *fft2* as in (14). G(u,v) with dimension MG x NG for each colour component is obtained as dot product (.*) of F(u,v) and H(u,v) as in (15). Dot product implies that each element of G(u,v) is a product of corresponding elements of F(u,v) and H(u,v). Equation (15) is the Matlab implementation of (2). Although the noise term in (2) is neglected in (15) but the noise term is still present in (15) in the form of computational approximation errors.

Each component of g (MG x NG x 3) is formed by two-dimensional discrete Inverse Fourier Transform of G(u,v) using Matlab code *ifft2* as in (16). Equations (13), (14) and (15) are repeated for the three colour components using the same two-dimensional blurring function h(m,n). The dimensions of H, F, G and g are all corrected to MG x NG in

(13), (14), (15) and (16); it's required that Matrices in an equation should have the same dimensions.

$$H(u,v) = fft2(h, MG, NG) \qquad (13)$$

$$F(u,v) = fft2(f_{colour coomponent}, MG, NG) \qquad (14)$$

$$G(u,v) = F(u,v).*H(u,v) \qquad (15)$$

$$g_{colour component} = ifft2[G(u,v)] \qquad (16)$$

To evaluate the error introduced by any system or process, the value of Peak Signal to Noise Ratio (PSNR) is evaluated. $PSNR_c$ compares the true image f(MF x NF x 3) with equivalent size of the acquired image g_1(MF x NF x 3) as in (17) [1,3,6,7,35,38]. g is a MG x NG x 3 matrix. g_1 (MF x NF x 3) matrix extracted from g (MG x NG x 3) as illustrated in Fig 3. g is the bigger matrix while g_1 is the inner shaded matrix in Fig. 3.

$$PSNR_c = 10\log_{10}\left[\frac{255^2}{\frac{1}{3(MF)(NF)}\left[\sum_{m=1}^{MF}\sum_{n=1}^{NF}\sum_{t=1}^{3}(g_1(m,n,t)-f(m,n,t))^2\right]} \right] (17)$$
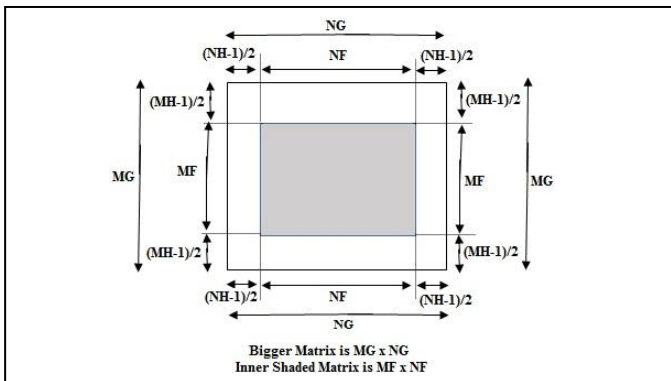

Figure 3. Extraction of MF x NF Matrix from MG x NG Matrix for each colour component.

D. Wiener Filter

h(m,n) of dimension MH x NH is transformed to frequency domain as H(u,v) of dimension MG x NG using the Matlab code *fft2* (Two-dimensional discrete Fourier Transform) as in (13). Conjugate of H(u,v) is evaluated using the Matlab code *conj* as in (18). Each of the three colour components of g (MG x NG x 3) is transformed to frequency domain as G(u,v) using Matlab code *fft2* as in (19). F_e(u,v) for each colour component is obtained as in (20) using the dot product (.*) and the dot division (./). Dot division is similar to dot product as explained in subsection C above. Equation (20) is the Matlab implementation of (7). Each component of restored image f_e(MG x NG x 3) is formed by two-dimensional discrete Inverse Fourier Transform using Matlab code *ifft2* as in (21). Each component of restored

image f_e obtainable in (21) is a MG x NG matrix but a MF x NF portion is extracted as illustrated in Fig. 3. f_e(MG x NG) is the bigger matrix while f_e(MF x NF) is the inner shaded matrix in Fig. 3.

$$H^*(u,v) = conj[H(u,v)] \qquad (18)$$

$$G(u,v) = fft2(g_{colour coomponent}, MG, NG) \qquad (19)$$

$$F_e(u,v) = [H^*(u,v).*G(u,v)]./[H^*(u,v).*H(u,v)+K] \quad (20)$$

$$f_{e\ colour\ component} = ifft2[F_e(u,v)] \qquad (21)$$

$PSNR_r$ compares the true image f(MF x NF x 3) with the restored image f_e(MF x NF x 3) as in (22). The Gain of the Wiener restoration filter is evaluated as in (23). The higher the Gain, the more efficient is the Wiener restoration process.

$$PSNR_r = 10\log_{10}\left[\frac{255^2}{\frac{1}{3(MF)(NF)}\left[\sum_{m=1}^{MF}\sum_{n=1}^{NF}\sum_{t=1}^{3}(f_e(m,n,t)-f(m,n,t))^2\right]} \right] (22)$$

$$Gain = PSNR_r - PSNR_c \qquad (23)$$

III. EXPERIMENTAL RESULTS AND DISCUSSIONS

A. Six Test Images

Six test images [39] are selected for testing the Wiener restoration filter. The Gain of the Wiener restoration filter using different values of parameter K (NSR) is evaluated for the six test images for various motion blur parameters Length (L) and direction (Angle θ). The test images are named as Clock, Car, Letter, Lena, Road, and Girl.

B. Effect of Variation of Parameter K (NSR) on Gain for constant Motion Blur Length and Direction

Clock was motion blurred with Length L=15 pixels and Angle θ=45°. Car was motion blurred with Length L=10 pixels and Angle θ=30°. Letter was motion blurred with Length L=15 pixels and Angle θ=45°. The motion blur parameters for the three test images were kept constant while Wiener filter parameter K (NSR) was varied. The Gain of the Wiener filter was evaluated and recorded for each value of parameter K for each of the three test images. The results are presented in Table V and plotted in Fig. 4. Tables VI, VII and VIII show the original or true image, the motion blurred image and restored images with different values of K for Clock, Car and Letter respectively.

As observed in Table V and Fig. 4, Wiener filter's Gain increases as K increases from 0 to a value termed 'Optimum K' when the Gain is maximum. The Gain reduces with further increase in K. Optimum K is determined experimentally and is indicated for each test image in Table

V and Fig. 4. As observed in Tables VI, VII and VIII, the visual appearance and quality of the restored image improve as K increases from 0 up to 'Optimum K'. The visual appearance and quality of the restored image decrease with further increase in K. At K = 0 when the Wiener filter is an inverse filter, the appearance and quality of the restored image are very poor with negative Gain. Thus, the output of an inverse filter is masked with amplified noise.

Lena was motion blurred with Length L=10 pixels and Angle θ=90°. Road was motion blurred with Length L=12 pixels and Angle θ=75°. Girl was motion blurred with Length L=8 pixels and Angle θ=135°. The original image, blurred image and optimum K restored image for Lena, Road and Girl are shown in Table IX. The optimum K for the restoration of Lena, Road and Girl are found to be 0.0012, 0.00045 and 0.0014 respectively with corresponding Gain of 8.794 dB, 10.527 dB and 7.943 dB respectively as presented in Table IX.
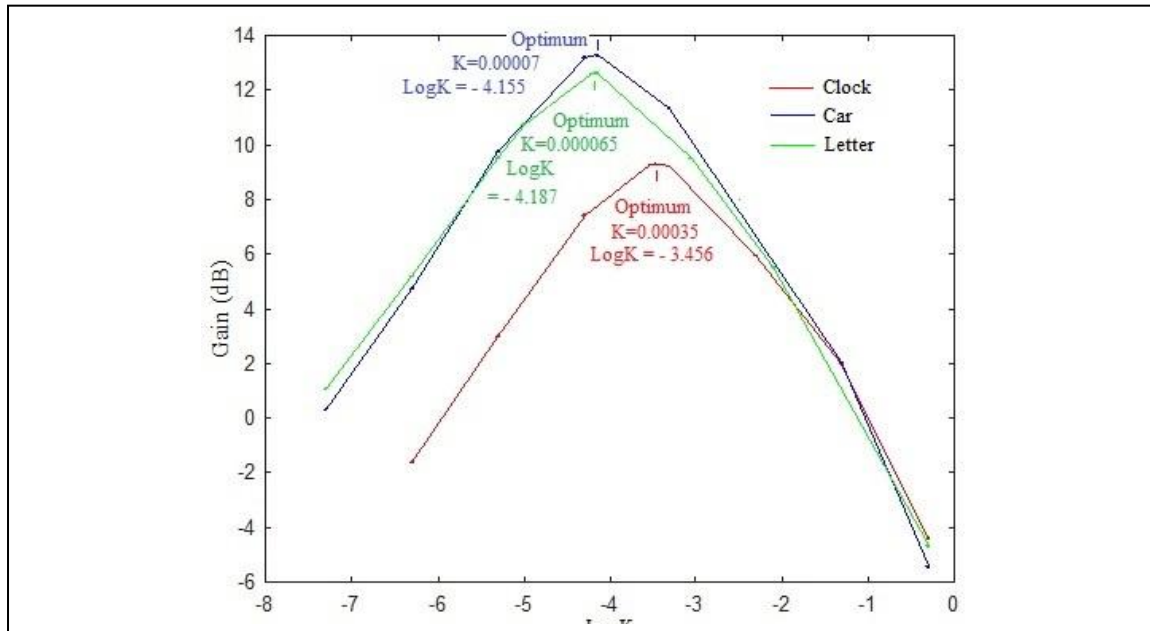

Figure 4.   Variation of Gain with LogK for three test images with constant motion blur length and direction.

TABLE V.   GAIN FOR DIFFERENT VALUES OF PARAMETER K (NSR) WITH CONSTANT MOTION BLUR LENGTH AND DIRECTION FOR CLOCK, CAR AND LETTER

Clock					Car					Letter				
Motion Blur Length L=15 pixcels & Angle = 45 degrees					Motion Blur Length L=10 pixcels & Angle = 30 degrees					Motion Blur Length L=20 pixcels & Angle = 10 degrees				
K	LogK	PSNRc (dB)	PSNRr (dB)	Gain (dB)	K	LogK	PSNRc (dB)	PSNRr (dB)	Gain (dB)	K	LogK	PSNRc (dB)	PSNRr (dB)	Gain (dB)
0	inf	21.945	5.7256	-16.22	0	inf	16.289	8.6399	-7.649	0.000	inf	14.097	4.954	-9.143
0.0000005	-6.301	21.945	20.344	-1.601	0.00000005	-7.301	16.289	16.616	0.327	0.00000005	-7.301	14.097	15.172	1.075
0.000005	-5.301	21.945	24.946	3.001	0.0000005	-6.301	16.289	21.037	4.748	0.0000005	-6.301	14.097	19.294	5.198
0.00005	-4.301	21.945	29.379	7.434	0.000005	-5.301	16.289	26.064	9.775	0.000005	-5.301	14.097	23.624	9.527
0.0003	-3.523	21.945	31.228	9.283	0.00005	-4.301	16.289	29.496	13.207	0.00001	-5.000	14.097	24.852	10.756
0.00035	**-3.456**	**21.945**	**31.239**	**9.294**	0.000069	-4.161	16.289	29.564	13.275	0.00006	-4.222	14.097	26.706	12.610
0.0004	-3.398	21.945	31.228	9.283	**0.00007**	**-4.155**	**16.289**	**29.565**	**13.276**	**0.000065**	**-4.187**	**14.097**	**26.714**	**12.618**
0.0005	-3.301	21.945	31.158	9.214	0.000071	-4.149	16.289	29.565	13.275	0.00007	-4.155	14.097	26.713	12.616
0.005	-2.301	21.945	27.902	5.957	0.0005	-3.301	16.289	27.628	11.339	0.0009	-3.046	14.097	23.603	9.507
0.05	-1.301	21.945	23.927	1.982	0.05	-1.301	16.289	18.338	2.049	0.008	-2.097	14.097	19.624	5.528
0.5	-0.301	21.945	17.551	-4.393	0.5	-0.301	16.289	10.857	-5.432	0.5	-0.301	14.097	9.421	-4.676

The rows with bold elements correspond to maximum Gain at optimum K.

TABLE VI.   RESTORED IMAGES FOR DIFFERENT VALUES OF PARAMETER K (NSR) WITH CONSTANT MOTION BLUR LENGTH AND DIRECTION FOR CLOCK
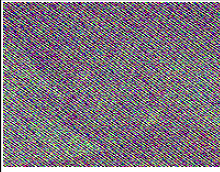
Clock (Original)	Clock (Blurred)	Clock (Restored) No. 1	Clock (Restored) No. 2
	L = 15 pixels & θ = 45 degrees PSNRc = 21.945 dB	PSNRr = 5.726 dB Gain = - 16.219 dB K= 0	PSNRr = 20.344 dB Gain = - 1.600 dB K= 0.0000005
Clock (Restored) No. 3	Clock (Restored) No. 4	Clock (Restored) No. 5	Clock (Restored) No. 6
PSNRr = 24.946 dB Gain = 3.000 dB K= 0.000005	PSNRr = 29.379 dB Gain = 7.434 dB K= 0.0000005	PSNRr = 31.228 dB Gain = 9.283 dB K= 0.0003	PSNRr = 31.239 dB **Gain = 9.294 dB** **Optimum K= 0.00035**
Clock (Restored) No. 7	Clock (Restored) No. 8	Clock (Restored) No. 9	Clock (Restored) No. 10
PSNr = 31.228 dB Gain = 9.283 dB K= 0.0004	PSNRr = 31.159 dB Gain = 9.214 dB K= 0.0005	PSNRr = 27.902 dB Gain = 5.957 dB K= 0.005	PSNRr = 17.551 dB Gain = - 4.394 dB K= 0.5

TABLE VII.   RESTORED IMAGES FOR DIFFERENT VALUES OF PARAMETER K (NSR) WITH CONSTANT MOTION BLUR LENGTH AND DIRECTION FOR CAR
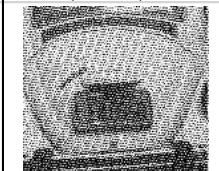
Car (Original)	Car (Blurred)	Car (Restored) No. 1	Car (Restored) No. 2
	L = 10 pixels & θ = 30 degrees PSNRc = 16.289 dB	PSNRr = 8.640 dB Gain = -7.649 dB K= 0	PSNRr = 16.616 dB Gain = 0.327 dB K= 0.00000005
Car (Restored) No. 3	Car (Restored) No. 4	Car (Restored) No. 5	Car (Restored) No. 6
PSNRr = 21.037 dB Gain = 4.748 dB K= 0.0000005	PSNRr = 26.064 dB Gain = 9.775 dB K= 0.000005	PSNRr = 29.496 dB Gain = 13.207 dB K= 0.00005	PSNRr = 29.564 dB Gain = 13.275 dB K= 0.000069
Car (Restored) No. 7	Car (Restored) No. 8	Car (Restored) No. 9	Car (Restored) No. 10
PSNRr = 29.565 dB **Gain = 13.276 dB** **Optimum K= 0.00007**	PSNRr = 29.565 dB Gain = 13.276 dB K= 0.000071	PSNRr = 18.338 dB Gain = 2.049 dB K= 0.05	PSNRr = 10.857 dB Gain = - 5.432 dB K= 0.5

TABLE VIII.   RESTORED IMAGES FOR DIFFERENT VALUES OF PARAMETER K (NSR) WITH CONSTANT MOTION BLUR LENGTH AND DIRECTION FOR LETTER
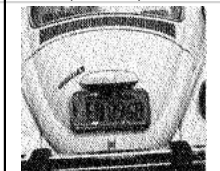
Letter (Original)	Letter (Blurred)	Letter (Restored) No. 1	Letter (Restored) No. 2
	L = 20 & θ = 15 degrees	PSNR 4.936 dB	PSNR 15.172 dB
	PSNR 14.097 dB	Gain = -9.143 dB	Gain = 1.075 dB
		K= 0	K= 0.00000005
Letter (Restored) No. 3	Letter (Restored) No. 4	Letter (Restored) No. 5	Letter (Restored) No. 6
PSNR 19.295 dB	PSNR 23.624 dB	PSNR 24.852 dB	PSNR 26.707 dB
Gain = 5.198 dB	Gain = 9.527 dB	Gain = 10.756 dB	Gain = 12.610 dB
K= 0.0000005	K= 0.000005	K= 0.00005	K= 0.00006
Letter (Restored) No. 7	Letter (Restored) No. 8	Letter (Restored) No. 9	Letter (Restored) No. 10
PSNR 26.7140 dB	PSNR 26.713 dB	PSNR 19.625 dB	PSNR 9.421 dB
Gain = 12.618 dB	Gain = 12.617 dB	Gain = 5.528 dB	Gain = - 4.676 dB
Optimum K= 0.000065	K= 0.00007	K= 0.008	K= 0.5

TABLE IX.   RESTORED IMAGES AT OPTIMUM K FOR LENA, ROAD AND GIRL

Lena (Original)	Lena (Blurred)	Lena (Restored at Optimum K)	Details
			L = 10 pixels & θ = 90 degrees
			Blurred Image PSNRc = 25.891 dB
			Restored Image PSNRr = 34.685 dB
			Gain at Optimum K = 8.794 dB
			Optimum K = 0.0012
Road (Original)	Road (Blurred)	Road (Restored at Optimum K)	Details
			L = 12 pixels & θ = 75 degrees
			Blurred Image PSNRc = 20.672 dB
			Restored Image PSNRr = 31.199 dB
			Gain at Optimum K = 10.527 dB
			Optimum K = 0.00045
Girl (Original)	Girl (Blurred)	Girl (Restored at Optimum K)	Details
			L = 8 pixels & θ = 135 degrees
			Blurred Image PSNRc = 27.942 dB
			Restored Image PSNRr = 35.885 dB
			Gain at Optimum K = 7.943 dB
			Optimum K= 0.0014

C. Effect of Variation of Motion Blur Direction on Optimum K (NSR) and Gain for Constant Motion Blur Length

The Optimum K and the corresponding Gain were determined and recorded in Table X for Clock, Car and Letter with constant motion blur length L=10 pixels and for various motion blur direction θ = 0°, 15°, 30°, 45°,…, 345°, 360°. The graph of Log of Optimum K versus motion blur direction θ is shown in Fig. 5 while Fig. 6 shows the graph of Gain at Optimum K versus motion blur direction θ.

TABLE X. OPTIMUM K AND GAIN FOR DIFFERENT VALUES OF MOTION BLUR DIRECTION WITH CONSTANT MOTION BLUR LENGTH FOR CLOCK, CAR AND LETTER

θ	Clock			Car			Letter		
	Optimum K	Log of Optimum K	Gain at Optimum K	Optimum K	Log of Optimum K	Gain at Optimum K	Optimum K	Log of Optimum K	Gain at Optimum K
0	0.00067	-3.174	8.127	0.00019	-3.721	9.822	0.0001	-4.000	12.097
15	0.0006	-3.222	8.877	0.000161	-3.793	12.940	0.00011	-3.959	13.794
30	0.00047	-3.328	9.290	0.00007	-4.155	13.276	0.000085	-4.071	13.592
45	0.00035	-3.456	9.294	0.00007	-4.155	14.754	0.000075	-4.125	14.320
60	0.00041	-3.387	9.563	0.00007	-4.155	13.755	0.0001	-4.000	12.987
75	0.00046	-3.337	9.142	0.000081	-4.092	12.634	0.00011	-3.959	11.849
90	0.00064	-3.194	7.814	0.000081	-4.092	12.006	0.00013	-3.886	10.549
105	0.0005	-3.301	8.783	0.000078	-4.108	12.664	0.00011	-3.959	11.980
120	0.00046	-3.337	9.366	0.000072	-4.143	13.744	0.00009	-4.046	12.972
135	0.00045	-3.347	9.728	0.000075	-4.125	14.790	0.000073	-4.137	14.197
150	0.00048	-3.319	8.972	0.000077	-4.114	13.715	0.000082	-4.086	13.886
165	0.00062	-3.208	8.814	0.00014	-3.854	13.018	0.0001	-4.000	13.730
180	0.00067	-3.174	8.128	0.00019	-3.721	9.822	0.0001	-4.000	12.097
195	0.0006	-3.222	8.877	0.000161	-3.793	12.940	0.00011	-3.959	13.794
210	0.00047	-3.328	9.290	0.00007	-4.155	13.276	0.000085	-4.071	13.592
225	0.00035	-3.456	9.294	0.00007	-4.155	14.754	0.000075	-4.125	14.320
240	0.00041	-3.387	9.563	0.00007	-4.155	13.755	0.0001	-4.000	12.987
255	0.00046	-3.337	9.142	0.000081	-4.092	12.634	0.00011	-3.959	11.849
270	0.00064	-3.194	7.814	0.000081	-4.092	12.006	0.00013	-3.886	10.549
285	0.0005	-3.301	8.783	0.000078	-4.108	12.664	0.00011	-3.959	11.980
300	0.00046	-3.337	9.366	0.000072	-4.143	13.744	0.00009	-4.046	12.972
315	0.00045	-3.347	9.728	0.000075	-4.125	14.790	0.000073	-4.137	14.197
330	0.00048	-3.319	8.972	0.000077	-4.114	13.715	0.000082	-4.086	13.886
345	0.00062	-3.208	8.814	0.00014	-3.854	13.018	0.0001	-4.000	13.730
360	0.00067	-3.174	8.128	0.00019	-3.721	9.822	0.0001	-4.000	12.097

L is kept constant at L = 10 pixels while θ is varied.

As observed in Table X and Fig. 5, Optimum K is exactly the same value for both θ and θ+180°. Similarly, as observed in Table X and Fig. 6, Gain at Optimum K is exactly the same value for both θ and θ+180°. The graph of both Log of Optimum K and Gain at Optimum K between 0° to 180° is repeated between 180° and 360°. This implies that motion blur functions of same length but of opposite direction are equivalent as they have the same effect on image and has the same potential for Wiener image restoration.

Optimum K decreases as θ varies from 0° to 45°; it increases as θ varies from 45° to 90°; it decreases as θ varies from 90° to 135°; it increases as θ varies from 135° to 180°. The cycle is then repeated between 180° and 360°.

Gain at Optimum K increases as θ varies from 0° to 45°; it decreases as θ varies from 45° to 90°; it increases as θ

varies from 90° to 135°; it decreases as θ varies from 135° to 180°. The cycle is then repeated between 180° and 360°.
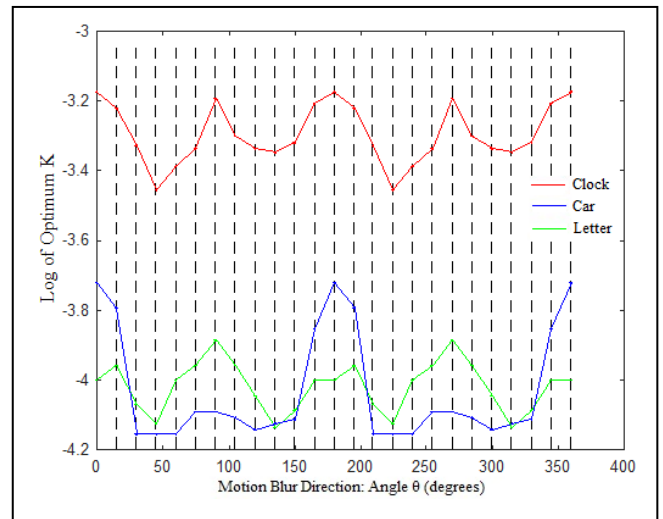

Figure 5. Variation of Log of Optimum K with motion blur direction (Angle θ) for three test images with constant motion blur length L=10 pixels.
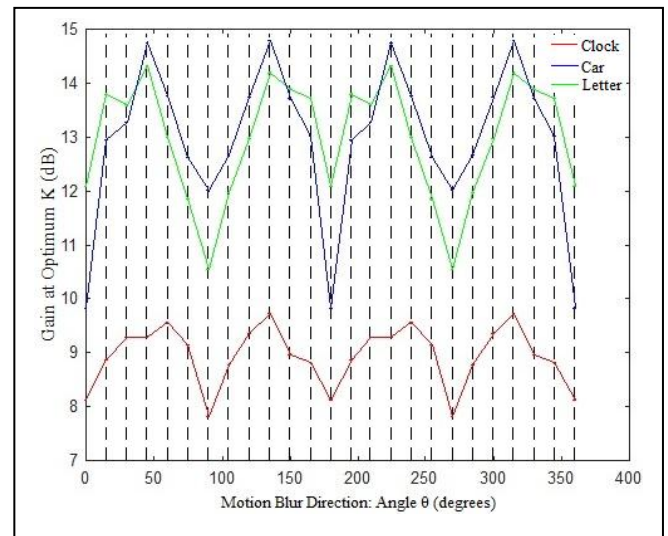

Figure 6. Variation of Log of Optimum K with motion blur direction (Angle θ) for three test images with constant motion blur length L=10 pixels.

D. Effect of Variation of Motion Blur Length on Optimum K (NSR) and Gain for Constant Motion Blur Direction

The Optimum K and the corresponding Gain were determined and recorded in Table XI for Clock, Car and Letter with constant motion blur direction θ = 45° and for various motion blur length L = 2, 5, 10, 15, 20 and 25 pixels. The graph of Log of Optimum K versus motion blur length L is shown in Fig. 7 while Fig. 8 shows the graph of Gain at Optimum K versus motion blur length L. Optimum K and Gain at Optimum K reduces as Length L increases from L = 2 pixels to at least L = 15 pixels.

TABLE XI. OPTIMUM K AND GAIN FOR DIFFERENT VALUES OF MOTION BLUR LENGTH WITH CONSTANT MOTION BLUR DIRECTION FOR CLOCK, CAR AND LETTER

Length L	Clock			Car			Letter		
	Optimum K	Log of Optimum K	Gain at Optimum K	Optimum K	Log of Optimum K	Gain at Optimum K	Optimum K	Log of Optimum K	Gain at Optimum K
2	0.00131	-2.883	14.408	0.0011	-2.959	20.998	0.00025	-3.602	21.720
5	0.00045	-3.347	9.804	0.00007	-4.155	14.687	0.00011	-3.959	14.617
10	0.0004	-3.398	9.968	0.00007	-4.155	14.754	0.000075	-4.125	14.320
15	0.00035	-3.456	9.294	0.00004	-4.398	12.805	0.000065	-4.187	13.504
20	0.0004	-3.398	8.136	0.000085	-4.071	11.282	0.000065	-4.187	11.537
25	0.00039	-3.409	8.235	0.00008	-4.097	12.283	0.000075	-4.125	12.276

θ kept constant at θ = 45° while L is varied.
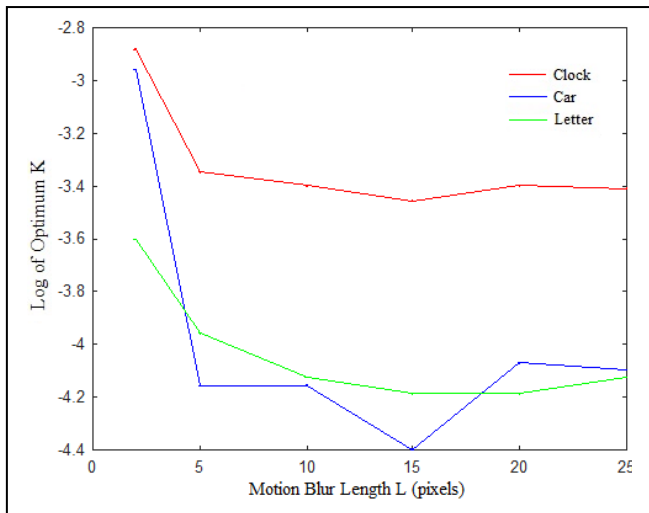

Figure 7.   Variation of Log of Optimum K with motion blur length L for three test images with constant motion blur direction θ =45°.
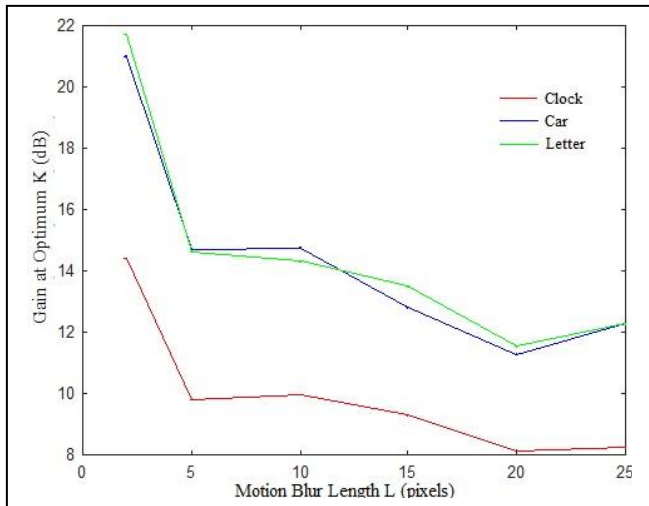

Figure 8.   Variation of Gain at Optimum K with motion blur length L for three test images with constant motion blur direction θ =45°.

IV.   CONCLUSION

Image degradation model, motion blur model and frequency domain restoration by Wiener filter have been extensively studied via experimental approach on six test images. The effects of motion blur parameters, Length and Direction, on Wiener filter's restoration quality, Gain and parameter K (Noise to Signal Ratio) have been investigated.

With constant motion blur parameters, Wiener filter's Gain and restoration quality are found to increase as K increases from 0 to a value termed Optimum K when the Gain is maximum and restoration quality is the best. Further increment in K beyond Optimum K decreases Gain and restoration quality. When K equals 0, the restored images were masked with amplified noise and the Wiener filter functioned as an inverse filter.

With constant motion blur length, Wiener filter's Optimum K and Gain at Optimum K are found to rise and fall rhythmically as motion blur direction varies from 0° to 180°. The variation patterns of Wiener filter's Optimum K and Gain at Optimum K as motion blur direction varies between 0° to 180° are exactly repeated as motion blur direction varies between 180° to 360°. Motion blur functions of same length but opposite directions are found to be equivalent. With constant motion blur direction, Wiener filter's Optimum K and Gain at Optimum K are found to decrease as motion blur length increases from 2 pixels to 15 pixels.

REFERENCES

[1] R. C. Gonzalez and R. E. Woods, Digital Image Processing. India: Prentice-Hall, 2007.

[2] T. F. Chan and J. Shen, Image Processing and Analysis: Variational, PDE, Wavelet and Stochastic Methods. Philadelphia, USA: SIAM, 2005.

[3] B. Chanda and D. D. Majumer, Digital Image Processing and Analysis. India: Prentice-Hall, 2000.

[4] R. C. Kenneth, Digital Image Processing. India: Prentice-Hall, 1996.

[5] I. T. Young, J. J. Gerbrands and L. J. van Vliet, Fundamentals of Image Processing. Netherlands: Delft University of Technology, 1998.

[6] A. R. Weeks, Fundamentals of Electronic Image Processing. India: Prentice-Hall, 1999.

[7] A. K. Jain, Fundamentals of Digital Image Processing. India: Prentice-Hall, 2003.

[8] F. C. Tony and S. Jianhong, Image Processing and Analysis: Variational, PDE, Wavelet, and Stochastic Methods. Philadelphia: SIAM, 2005.

[9] A. S. Carasso, "Linear and Nonlinear Image Deblurring: A documented study," SIAM Journal on Numerical Analysis, vol. 36, pp. 1659–1689, 1999.

[10] L. Yang, "Image Restoration from a Single Blurred Photograph," 3rd Int. Conf. on Information Science and Control Engineering (ICISCE), pp. 405-409, 2016.

[11] M. R. Banham and A. K. Katsaggelos, "Digital Image Restoration," IEEE Signal Processing Magazine, vol. 14, no. 2, pp. 24–41, 1997.

[12] Y. H. Fung and Y. H. Chan, "An Iterative Algorithm for Restorating Colour-Quantized Image,". Proc. ICIP, vol. 1, pp. 313–316, 2002.

[13] M. Trimeche, D. Paliy, M. Vehvilainen and V. Katkovnik, "Multichannel image deblurring of raw color components," Proceedings of SPIE 5674, pp. 169-178, 2005.

[14] G. B. Giannakis, W. Robert and R. W. Heath, "Blind Identification of Multichannel FIR Blurs and Perfect Image Restoration," IEEE Trans. on Image Processing, vol. 9 no. 11, pp. 1877-1896, 2000.

[15] H. Yamauchi, J. Haber and H. P. Seidel, "Image Restoration using Multiresolution Texture Synthesis and Image Inpainting," Computer Graphics International, pp. 108-113, 2003.

[16] M. G. Kang and A. K. Katsaggelos, "General choice of the regularization functional in regularized image restoration," IEEE Trans. Image Processing, vol. 4, no. 5, pp. 594–602, 1995.

[17] S. H. Lee, N. I. Cho and J. Park, "Directional Regularisation for Constrained Iterative Image Restoration," Electronics Letters, vol. 39, no. 23, pp. 1642-1643, 2003.

[18] W. Zhu, Y. Wang, J. Chang, H. L. Graber and R. Barbour, "A Total Least Squares Approach for the Solution of The Perturbation Equation. J. Optical Soc. Am. A, vol. 14, no. 4, 1977.

[19] M. Bertero and P. Boccacci, Introduction to Inverse Problem in Imaging. Bristol: IOP Publishing Ltd., 1998.

[20] M. Bertero, and P. Boccacci, Inverse Problems and Computational Imaging. Encyclopedia of Modern Optics, eds. R. D. Guenther, D. G. Steel, and L. Bayvel, vol. 2, pp. 118-127, 2004 ().

[21] Mosegaard, K. (1995). Monte Carlo sampling of solutions to inverse problems. Journal of Geophysical Research, Vol. 100(No. B7), pp. 12431–12447.

[22] A. R. Zubair, "Comparison of Image Enhancement Techniques," International Journal of Research in Commerce, IT & Management, vol. 2, no. 5, pp. 44-52, 2012.

[23] J. H. Pujar and K. S. Kunnur, "A Novel Approach for Image Restoration via Nearest Neighbour Method," Journal of Theoretical and Applied Information Technology, vol. 14, no. 2, 2010.

[24] Z. Al-Ameen, D. Mohamad, M. Shafry, M. R. Sulong and G. Sulong, "Restoring Degraded Astronomy Images using a Combination of Denoising and Deblurring Techniques," International Journal of Signal Processing, Image Processing and Pattern Recognition (IJSIP), vol. 5, no. 1, 2012.

[25] M. N. Hussien and M. I. Saripan, "Computed Tomography Soft Tissue Restoration using Wiener Filter," Proceedings of 2010 IEEE Student Conference on Research and Development (SCOReD), pp. 415 - 420, 2010.

[26] Z. Mbarki, H. Seddik and E. B. Braiek, "A rapid hybrid algorithm for image restoration combining parametric Wiener filtering and wave atom transform," J. Visual Communication and Image Representation, vol 40, part B, pp. 694-707, 2016.

[27] A. Khireddine, K. Benmahammed and W. Puech, "Digital image restoration by Wiener filter in 2D case," Advances in Engineering Software, vol. 38, no. 7, pp.513–516, 2007.

[28] A. M. Deshpande and S. Patnaik, "Comparative Study and Qualitative-Quantitative Investigations of Several Motion Deblurring Algorithms," IJCA Proceedings on International Conference and workshop on Emerging Trends in Technology (ICWET), vol. 2, pp. 27-34, 2011.

[29] K. Kondo, Y. Ichioka, and T. Suzuki, "Image restoration by Wiener filtering in the presence of signal-dependent noise," Applied Optics vol. 16, no. 9, pp. 2554-2558, 1977.

[30] S. Lahmiri, M. Boukadoum, "Hybrid Wiener and partial differential equations filter for biomedical image denoising," 14th IEEE New Circuits and Systems Conference (NEWCAS), pp. 1-4, 2016.

[31] S. Trambadia and P. Dholakia, "Design and analysis of an image restoration using wiener filter with a quality based hybrid algorithms," 2nd International Conference on Electronics and Communication Systems (ICECS), pp. 1318-1323, 2015.

[32] J. Yoo and C. W. Ahn, "Image restoration by blind-Wiener filter," IET Image Processing,, vol. 8, no. 12, pp. 815 – 823, 2014.

[33] N. Kumar and K. K. Singh, "Wiener filter using digital image restoration," Int. J. Electron. Eng., vol. 3, no. 2, pp. 345-348, 2011.

[34] H. Furuya, S. Eda and T. Shimamura, "Image restoration via Wiener filtering with improved noise estimation," ISPRA'09 Proceedings of the 8th WSEAS international conference on Signal processing, robotics and automation, pp. 315-320, 2009.

[35] A. R. Zubair, "Spatial Domain Restoration Scheme," Proceedings of the Fourth International Conference on Research and Development, vol. 4, no. 8: 46-54, 2011.

[36] MathWorks Product Documentation Files, R2011b, "Documentation, Image Processing Toolbox, fspecial function help file," http://www.mathworks.com/help/toolbox/images/ref/fspecial.html, 2011.

[37] R. C. Gonzalez, R. E. Wood and S. L. Eddin, Digital Image Processing Using MATLAB. USA: Pearson Prentice-Hall, 2004.

[38] S. S. O. Choy, Y. Chan and W. Siu, "An Improved Quantitative Measure of Image Restoration Quality," Proc. IEEE International Confeence on Acoustics, Speech and Signal Processing (ICASSP'96), vol. III, pp. 1613-1616, 1996.

[39] USC-SIPI Image Database (2006), Standard Test Images retrieved on October 5, 2006 from the database of Signal and Image Processing Institute of the University of Southern California, USA: http://sipi.usc.edu/database/index.html